FEBS Open Bio 2 (2012) 60–70

FEBS openbio

journal homepage: www.elsevier.com/locate/febsopenbio

Kinetic and thermodynamic analysis of the conformational folding process of SS-reduced bovine pancreatic ribonuclease A using a selenoxide reagent with high oxidizing ability

Kenta Arai, Fumio Kumakura, Michio Iwaoka *

Department of Chemistry, School of Science, Tokai University, Kitakaname, Hiratsuka-shi, Kanagawa 259-1292, Japan

ARTICLE INFO

Article history:
Received 26 March 2012
Revised 10 April 2012
Accepted 10 April 2012

Keywords:
Oxidative protein folding
Selenoxide
Ribonuclease A
Disulfide bond
X-Pro isomerization
Trans-3,4-dihydroxyselenolane oxide

ABSTRACT

Redox-coupled folding pathways of bovine pancreatic ribonuclease A (RNase A) with four intramolecular disulfide (SS) bonds comprise three phases: (I) SS formation to generate partially oxidized intermediate ensembles with no rigid folded structure; (II) SS rearrangement from the three SS intermediate ensemble (3S) to the des intermediates having three native SS linkages; (III) final oxidation of the last native SS linkage to generate native RNase A. We previously demonstrated that DHS^{ox}, a water-soluble selenoxide reagent for rapid and quantitative SS formation, allows clear separation of the three folding phases. In this study, the main conformational folding phase (phase II) has been extensively analyzed at pH 8.0 under a wide range of temperatures (5–45 °C), and thermodynamic and kinetic parameters for the four des intermediates were determined. The free-energy differences (ΔG) as a function of temperature suggested that the each SS linkage has different thermodynamic and kinetic roles in stability of the native structure. On the other hand, comparison of the rate constants and the activation energies for 3S → des with those reported for the conformational folding of SS-intact RNase A suggested that unfolded des species (desU) having three native SS linkages but not yet being folded are involved in very small amounts (<1%) in the 3S intermediate ensemble and the desU species would gain the native-like structures via X-Pro isomerization like SS-intact RNase A. It was revealed that DHS^{ox} is useful for kinetic and thermodynamic analysis of the conformational folding process on the oxidative folding pathways of SS-reduced proteins.

1. Introduction

Understa

for de novo structurally characteristic intermediates, such as hydrophobic clusters [2–5], molten globules [6–8], and discrete structured mechanism for misfolded protein disorders caused by amyloid formation [2]. Previous experimental and theoretical achievements have demonstrated that the folding follows pathways through these quasi-stable folding intermediates is not easy because they are short-lived under the folding conditions. A redox-coupled oxidative folding method is frequently applied to the folding study of disulfide (SS)-containing proteins, for which the partially oxidized SS intermediates generated during the oxidative folding process can be trapped and isolated by controlling the folding conditions [12]. Small monomeric proteins, such as bovine pancreatic trypsin inhibitor (BPTI) [9,13], hen egg white lysozyme [11,14], α-lactalbumin [15], hirudin [16], and bovine pancreatic ribonuclease A (RNase A) [17], have been used as model proteins for oxidative folding study.

RNase A is a typical globular protein of 124 amino acid residues containing four SS bonds (C40–C95, C65–C72, C26–C84, and C58–C110) [18]. By using *trans*-4,5-dihydroxy-1,2-dithiane (DTT^{ox}) as an oxidant for SS formation, the major oxidative folding pathways from the fully reduced state (R) to the native state (N) have been well established by Scheraga and coworkers as shown in Fig. 1

Abbreviations: 1S, 2S, 3S, and 4S, ensembles of folding intermediates of RNase A with one, two, three, and four SS linkages, respectively; AEMTS, 2-aminoethyl methanethiosulfonate; BPTI, bovine pancreatic trypsin inhibitor; des[26–84], des[40–95], des[58–110], and des[65–72], structured 3S intermediates of RNase A having three native SS bonds but lacking one native SS bond specified; desN, folded des intermediate; desU, unfolded des intermediate; DHS^{ox}, *trans*-3,4-dihydroxyselenolane oxide; DTT^{red}, dithiothreitol; DTT^{ox}, oxidized DTT; EDTA, ethylenediaminetetraacetic acid; ESI, electron spray ionization; GSSG, oxidized glutathione; HEPES, 4-(2-hydroxyethyl)-1-piperazineethanesulfonic acid; HPLC, high performance liquid chromatography; N, native RNase A; R, reduced RNase A; RNase A, bovine pancreatic ribonuclease A; SH, thiol; SS, disulfide; TFA, trifluoroacetic acid; U, unfolded RNase A; UV, ultraviolet

* Corresponding author. Fax: +81 463 50 2094.
E-mail addresses: miwaoka@tokai.ac.jp, miwaoka@keyaki.cc.u-tokai.ac.jp (M. Iwaoka).

2211-5463
http://dx.doi.org/10.1016/j.fob.2012.04.001

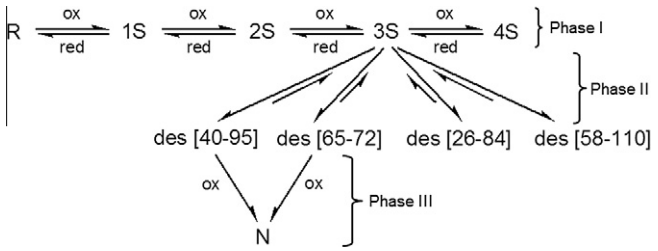

Fig. 1. Major oxidative folding pathways of RNase A. Phase I is the first SS formation phase (a chain-entropy losing phase), phase II is the second SS rearrangement phase (a conformational folding phase), and phase III is the final oxidation phase to generate the native state.

[19–21]. After initiation of the folding by addition of an excess amount of DTT^{ox}, R having no SS bond is gradually oxidized to the ensembles of 1S, 2S, 3S, and 4S intermediate species, which have one–four SS bonds, respectively. In this oxidation process, any rigid folded structures are not yet generated (phase I). Subsequently, the 3S intermediates are converted to the structured intermediates having three native SS bonds, i.e., des[40–95], des[65–72], des[26–84], and des[58–110], by slow intramolecular SH–SS exchange reaction (called here SS rearrangement) generating the native-like structures (phase II). Finally, des[40–95] and des[65–72] are oxidized to N by DTT^{ox} remaining in the reaction solution (phase III). Des[26–84] and des[58–110], which are kinetically trapped intermediates, can be observed only at low temperatures (<15 °C) and have not yet been isolated to investigate their folding behaviors because their populations were very low under previously applied oxidative folding conditions. In addition to the major folding pathways shown in Fig. 1, the oxidation from 2S to des[40–95] or des[65–72] has also been characterized as the minor folding pathways [22,23]. It should be noted that the 4S can be converted to N through the reduction to 3S by reacting with DTT^{red} existing in the solution.

In general, oxidative folding pathways of a protein with several SS bonds involve two basic reactions; SS formation (oxidation) and intramolecular SH–SS exchange reactions. The former corresponds to global packing of the polypeptide chain causing the entropy loss, and the latter corresponds to the rapid SS reshuffling or slow SS rearrangement to search for the conformations enthalpically stabilized by native or non-native interactions [12]. In the conventional methods, sulfur-containing oxidants, such as DTT^{ox} and oxidized glutathione (GSSG), are employed under weakly basic conditions (ca. pH 7–9) [9,11,13–17], which allow for competitive progress of the SS formation and SH–SS exchange reactions. Roles of the partially oxidized SS intermediates can be investigated by quenching the reactions by chemically modifying remaining SH groups [17,24,25] or by using engineered mutants of the SS intermediates [26–29]. Recently, new types of oxidative folding reagents, such as polymer-bound sulfur-containing compounds [30], aromatic sulfur compounds [31,32], platinum complexes [33,34], and diselenides [35,36], have been synthesized and examined. Protein disulfide isomerase [37,38] and short peptides with a –Cys–Xaa–Xaa–Cys– motif [39] have also been applied to the study of oxidative protein folding.

On the other hand, we recently demonstrated that a new approach using a water-soluble selenium-containing oxidant, *trans*-3,4-dihydroxyselenolane oxide (DHS^{ox}), is promising for elucidation of oxidative folding pathways of a protein more easily and more accurately [40]. Since DHS^{ox} has highly strong and selective oxidizing ability, it enables rapid, quantitative, and irreversible SS formation of the folding intermediates under wide pH conditions (ca. pH 3–10) [41,42]. Thus, by using DHS^{ox}, the SS formation process (phase I) can be cleanly separated from the slow SS rearrangement processes (phase II). In the oxidative folding of RNase A, des[40–95] and des[65–72] intermediates could be easily observed at 25 °C and pH 8.0 after addition of three equivalents of DHS^{ox} to R. Furthermore, it was evidenced that the SS formation (phase I) can be divided to two subphases; kinetic SS formation phase (phase Ia) and the thermodynamic SS reshuffling phase corresponding to redistribution of the SS intermediates to slightly stabilized SS species (phase Ib) [42]. The transition from the kinetic to thermodynamic phases by rapid SS reshuffling was reflected by hydrophobic clustering of the polypeptide chain accompanying generation of native interactions. The kinetic SS formation process (phase Ia) was further suggested to follow a stochastic reaction because the rate constants were roughly proportional to the number of the SH groups present along the polypeptide chain [40,42,43]. After generation of the thermodynamically stabilized SS intermediates via stochastic SS formation and rapid SS reshuffling, the folding moves to a subsequent conformational folding stage (phase II), where 3S intermediates are transformed to the des intermediates via slow SS rearrangement accompanying generation of the native-like structures.

In the present study, the SS rearrangement reaction (phase II) of RNase A from 3S to the des intermediates, which is a main process to build up the native structure, is focused. While all four possible des intermediates having discrete folded structures were previously observed as the key intermediates for oxidative folding of RNase A [19,20], their thermodynamic properties have not been quantitatively determined albeit the behaviors of analogous mutants, such as [C40S, C95S] and [C65S, C72S], have been extensively studied [28,29,44]. In the meantime, in the oxidative folding of SS-containing proteins, there is a controversial argument: which occurs earlier, formation of native SS linkages or acquisition of the native structure [45–49]? Scheraga and coworkers previously elucidated that in generation of des[40–95], the conformational folding coupled with X-Pro93 isomerization takes place after formation of the third native SS linkage on the basis of two experiments, i.e., the redox-coupled unfolding/folding of RNase A using the P93A mutant and the conformational folding of SS-intact des[40–95] [45,47]. However, it is not yet known whether this model is applicable to the other three des intermediates. On the other hand, Boudko and Engel demonstrated that in type III collagen the SH groups have to be properly placed for formation of the native SS bonds [48]. There are other instances, in which formation of native SS bonds is conducted by native structure formation [49].

Thermodynamic and kinetic behaviors of four des intermediates of RNase A have been extensively studied herein at pH 8.0 under a wide range of temperatures (5–45 °C) by applying DHS^{ox} as an oxidative folding reagent. The relative thermodynamic stabilities about the four des intermediates were quantitatively determined for the first time without use of the analogous mutants. The reaction rate constants for 3S → des were also clearly determined. On the basis of the obtained thermodynamic and kinetic parameters, roles of the each native SS linkage in stability of the native structure as well as a relation between the conformational folding processes of SS-intact RNase A and those of SS-reduced RNase A are discussed. Furthermore, we have succeeded in isolation of the four des intermediates by acid quenching of the folding mixture and subsequent fractionation by reverse-phase HPLC. The each isolated des intermediate was allowed to fold to N under an aerobic condition to confirm phase III of the folding pathways.

2. Materials and methods

2.1. Materials

RNase A (type 1-A) was purchased from Sigma–Aldrich, Japan, and used without purification. DHS^{ox} [50] and 2-aminoethyl meth-

anethiosulfonate (AEMTS) [51] were synthesized according to the literature methods. All other reagents were commercially available and used without further purification.

2.2. Preparation of reduced RNase A (R)

The experimental procedure previously described [40] was followed. To a solution of RNase A (4–7 mg) dissolved in 0.6 ml of a 100 mM Tris–HCl/1 mM EDTA buffer solution at pH 8.5 containing 4 M guanidine thiocyanate as a denaturant was added an excess amount of DTT^{red} (7–8 mg). The reaction mixture was incubated at room temperature for 50 min. Resulting R was purified by passing through the column packed with Sephadex G25 resin, which was equilibrated with a 100 mM Tris–HCl/1 mM EDTA buffer solution at pH 8.0 purged with nitrogen. The concentration of R obtained was determined by UV absorbance at 275 nm ($\varepsilon = 8600$ M^{-1} cm^{-1} [17]). The R solution was immediately used in the following folding experiments.

2.3. Oxidative folding of RNase A using DHS^{ox} as an oxidant

A DHS^{ox} solution in 100 mM Tris–HCl/1 mM EDTA buffer at pH 8.0 was prepared so that the concentration of DHS^{ox} was three-fold with respect to R. The R and DHS^{ox} solutions were maintained at 5.0, 15.0, 25.0, 35.0, or 45.0 ± 0.1 °C in a dry thermo bath. Two hundred micro-liters of the R solution was manually added with 200 μl of the DHS^{ox} solution in a 1.5 ml micro-centrifuge tube. The mixture was intensely stirred by vortexing for 5 s and was incubated for a certain period of time (1–1680 min) in a dry thermo bath regulated at 5.0–45.0 ± 0.1 °C.

Three sample solutions with a different post-oxidation treatment were prepared for each reaction time. The first sample solution was added with 200 μl of an aqueous AEMTS solution (7 mg/ml) to quench SS reshuffling and SS rearrangement reactions (without a redox pulse). AEMTS is a thiol blocking reagent that modifies a free SH group to $SSCH_2CH_2NH_3^+$ giving a polythiol molecule one unit of positive charge and 76 Da of molecular mass per one SH group. For the second sample solution, a reduction pulse was applied according to the literature [52]. Before quenching the reactions by addition of AEMTS, 200 μl of a 100 mM Tris–HCl/1 mM EDTA buffer solution at pH 8.0 containing 21–27 mM DTT^{red} (a reduction pulse) was added to the sample solution. After 2–4 min at the same temperature, the reaction was quenched with 400 μl of the aqueous AEMTS solution. For the third sample solution, an oxidation pulse was applied [21,34]. Before the AEMTS quenching, 200 μl of a 100 mM Tris–HCl/1 mM EDTA buffer solution at pH 8.0 containing DHS^{ox} of the same concentration as R (an oxidation pulse) was added to the sample solution. After 3 min at the same temperature, the reaction was quenched with 200 μl of the AEMTS solution. The collected sample solutions were acidified to pH 2–3 with 8 μl of 2 M acetic acid and stored at –30 °C.

In parallel to the above long-term folding experiments, recovery of the native structure of RNase A was monitored by UV spectroscopy at the same temperature. Five hundred micro-liters each of the R and DHS^{ox} solutions were mixed and poured into the 1 ml quartz cell, which was set in the cell holder of a Shimadzu UV-1700 spectrophotometer thermostated at 5.0, 15.0, 25.0, 35.0, or 45.0 ± 0.1 °C by using a circulating water-bath system.

2.4. Isolation and folding of des intermediates

Four des intermediates of RNase A were isolated by the following procedure. The folding sample solution (400 μl), which was obtained by addition of 3 eq DHS^{ox} to R and subsequent incubation at 5 °C for 15 h, was treated under a reduction pulse condition (200 μl of 27 mM DTT^{red}) at 5 °C for 4 min. The solution was then acidified with 25 μl of 15% aqueous trifluoroacetic acid (TFA) solution. The crude des products obtained were desalted by using a Sephadex G25 column into 0.1 M acetic acid and fractionated by HPLC equipped with a 1 ml sample solution loop and a Tosoh TSKgel ODS-100V 4.6 × 150 mm reverse-phase column, which was equilibrated with 74:26 (v/v) mixture of 0.1% TFA in water (eluent A) and 0.1% TFA in acetonitrile (eluent B) at a flow rate of 0.8 ml/min. A solvent gradient (a ratio of eluent B linearly increased from 26% to 28% in 0–35 min, from 28% to 55% in 35–40 min, from 55% to 55% in 40–45 min, from 55% to 100% in 45–46 min) was applied. The separated des intermediates were detected by UV absorption at 280 nm. Each isolated des intermediate was subsequently folded to N under an aerobic condition as follows. The fractionated solution was lyophilized and dissolved in 30 μl of 1 mM HCl at 4 °C. The pH of the solution was then increased by addition of 900 μl of 100 mM Tris–HCl/1 mM EDTA buffer solution at pH 8.0 and 5 °C in order to induce slow SS formation by air oxidation and SS reshuffling of the des intermediate. The mixture was incubated in a dry thermo bath regulated at 5.0 ± 0.1 °C. After a certain period of time (5–300 min), 100 μl of the aliquot was taken from the mixture into 200 μl of an aqueous AEMTS solution in a 1.5 ml microtube. After 5 min, the resulting sample solution was acidified to pH 2–3 with 8 μl of 2 M acetic acid and stored at –30 °C.

2.5. Temperature-jump experiments

The R and DHS^{ox} solutions with the concentration ratio of 1:3 were cooled at 15.0 ± 0.1 °C in a thermostated water bath. Five milliliters each of the solutions were mixed in a 15 ml micro-centrifuge tube. The mixture was rapidly stirred by vortexing for 10 s and incubated at 15.0 ± 0.1 °C in a thermostated water bath under nitrogen for 300 min. An aliquot (400 μl) of the reaction solution was taken out and reacted with 200 μl of an aqueous AEMTS solution (7 mg/ml) to quench the reaction. The temperature of the water bath was then increased to 25.0 ± 0.1 °C. After 20 min, an aliquot (400 μl) of the reaction solution was taken out and reacted with 200 μl of the AEMTS solution. Similarly, the temperature was further increased to 35.0 °C for 20 min and then decreased to 15.0 °C for 300 min. At each temperature an aliquot of the reaction solution was reacted with AEMTS. The collected sample solutions were acidified and stored at –30 °C.

2.6. HPLC analysis

The sample solutions from the above folding experiments were thawed and desalted by using a Sephadex G25 column equilibrated with 0.1 M acetic acid. The desalted solutions were analyzed by HPLC according to the method described previously [40]. A Shimadzu VP series high performance liquid chromatograph system equipped with a 5 ml sample solution loop and a Tosoh TSKgel SP-5PW cation-exchange 75 × 7.5 column was used. After sample injection, a Na_2SO_4 gradient was applied by linearly increasing the ratio of buffer B from 0% to 45% in 50 min at a flow rate of 0.5 ml/min: buffer A was 25 mM HEPES/1 mM EDTA at pH 7.0 and buffer B was buffer A + 0.5 M Na_2SO_4. The folding intermediates were detected by UV absorption at 280 nm. The recorded signals were integrated and analyzed by using a Shimadzu LC solution software.

2.7. Characterization of folding intermediates

The AEMTS-quenched folding intermediates fractionated by HPLC were collected, purified by using a Sephadex G25 column into 0.1 M acetic acid, and lyophilized. The molecular mass of each intermediate was measured on a Jeol JMS-T100LP spectrometer

connected to an Agilent 1200 series HPLC system. For four des intermediates, the collected sample was digested by trypsin and α-chymotrypsin and analyzed by using the LC-MS system to identify the SS bonds according to the literature method [40,53].

3. Results

3.1. Oxidative folding of RNase A at various temperatures

When R was reacted with three equivalents of DHS^{ox} as an oxidant at pH 8.0 for 1 min, 1S–4S folding intermediates were obtained with 3S as major products as previously reported [40]. According to profiles of the HPLC chromatograms, the same intermediate ensembles with SS components were observed in a range of the reaction temperature between 5 and 45 °C. However, the intermediates produced after 3 h became significantly different from each other depending on the incubation temperature as seen in the HPLC chromatograms shown in Fig. 2.

At low temperatures (i.e., at 5 and 15 °C), growth of five distinct peaks was observed (Fig. 2a and b). These peaks were unambiguously assigned to native RNase A (N) having four native SS bonds and four des intermediates (des[65–72], des[58–110], des[26–84], and des[40–95], respectively) by ESI(+)-MS analysis of the samples collected from the HPLC elutant as well as by the SS-bond analysis applying the trypsin and α-chymotrypsin digestion method. Since the des intermediates were not obviously observed when two or four equivalents of DHS^{ox} were employed, they should be mainly generated from the 3S intermediates via slow intramolecular SS rearrangement. Formation of N would be achieved by oxidation of des[65–72] and des[40–95] through intermolecular SH–SS exchange reactions [54].

When similar long-term folding experiments were carried out at 25 °C, populations of des[58–110] and des[26–84] decreased significantly, while des[65–72] and des[40–95] could be seen clearly in the HPLC chromatogram (Fig. 2c). The des[40–95] and des[65–72] intermediates, however, disappeared apparently at 35 and 45 °C, respectively (Fig. 2d and e). The observation strongly suggested that each des intermediate has different thermodynamic stability.

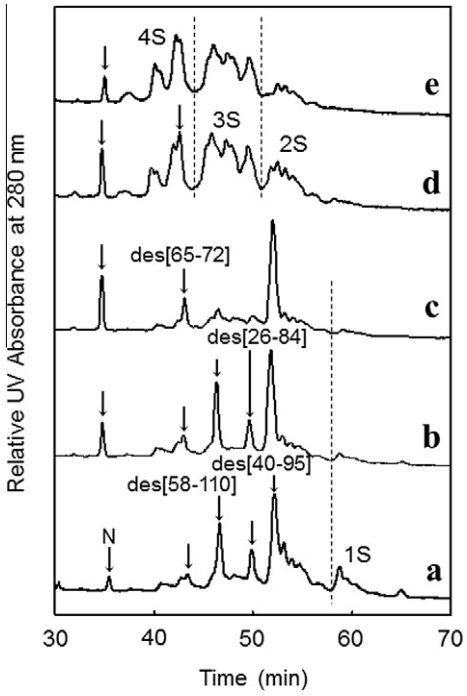

Fig. 2. HPLC chromatograms obtained by the long-term folding experiments of RNase A using three equivalents of DHS^{ox} as an oxidant at pH 8.0 and 5–45 °C. The refolding time was 180 min. Reaction conditions: (a) $[R]_0 = [DHS^{ox}]_0/3 = 19.4$ μM at 5 °C; (b) $[R]_0 = [DHS^{ox}]_0/3 = 20.7$ μM at 15 °C; (c) $[R]_0 = [DHS^{ox}]_0/3 = 24.7$ μM at 25 °C; (d) $[R]_0 = [DHS^{ox}]_0/3 = 21.3$ μM at 35 °C; (e) $[R]_0 = [DHS^{ox}]_0/3 = 24.2$ μM at 45 °C. See the text for details of the HPLC analysis conditions.

3.2. Equilibriums between 3S and the des intermediates

Reversible interconversion between the 3S and four des intermediates was confirmed by the temperature-jump experiment (Fig. 3). When the folding solution obtained by the reaction of R with three equivalents of DHS^{ox} at 15 °C for 5 h was allowed to be maintained at 25 °C for 20 min, populations of des[26–84] and des[58–110] were reduced, while the population of 3S was enhanced. Subsequent treatment of the solution at 35 °C for 20 min caused a decrease in the population of des[40–95] and an increase in the population of 3S. These population changes were almost completely retrieved when the solution was maintained at 15 °C for 5 h again. Thus, the presence of the equilibriums shown in Eqs. (1)–(4) is evident.

$$3S \underset{k_1^r}{\overset{k_1^f}{\rightleftharpoons}} \text{des}[40\text{—}95] \quad (1)$$

$$3S \underset{k_2^r}{\overset{k_2^f}{\rightleftharpoons}} \text{des}[65\text{—}72] \quad (2)$$

$$3S \underset{k_3^r}{\overset{k_3^f}{\rightleftharpoons}} \text{des}[26\text{—}84] \quad (3)$$

$$3S \underset{k_4^r}{\overset{k_4^f}{\rightleftharpoons}} \text{des}[58\text{—}110] \quad (4)$$

3.3. Reduction pulse

To get more quantitative information about populations of the four des intermediates as a function of the reaction time at various temperatures, a reduction pulse of DTT^{red} [52] was applied to the

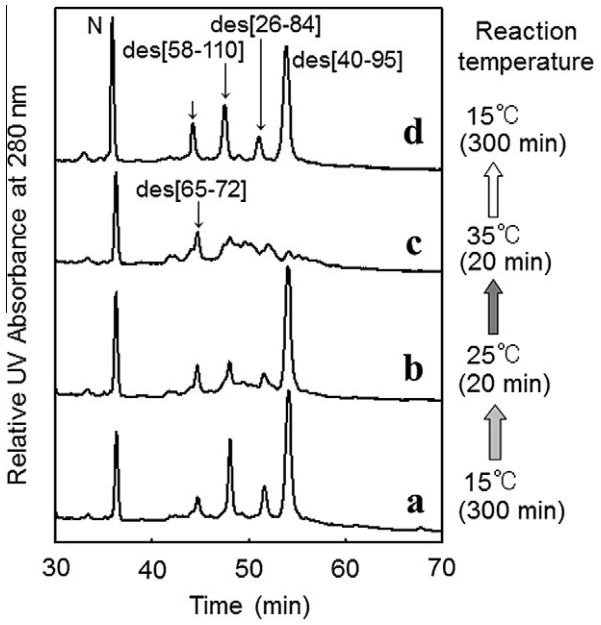

Fig. 3. HPLC chromatograms obtained by the temperature-jump experiment for the folding intermediates of RNase A generated by the reaction of R with three equivalents of DHS^{ox} at pH 8.0. Reaction conditions: $[R]_0 = [DHS^{ox}]_0/3 = 19.0$ μM. (a) Incubated at 15 °C for 300 min. (b) Incubated at 25 °C for 20 min after (a). (c) Incubated at 35 °C for 20 min after (b). (d) Incubated at 15 °C for 300 min after (c). See the text for details of the HPLC analysis conditions.

sample solutions containing oxidative folding intermediates of RNase A. Addition of the reductant with a high concentration should rapidly reduce the folding intermediates (i.e., 1S–4S) back to R (and/or 1S) except for the intermediates having robust folded structures, which sterically prevent the SS bonds from an attack of the reductant. Thus, by application of a reduction pulse the intermediates having folded structures could be easily identified among a number of the oxidative folding intermediates, and their exact populations were determined.

The HPLC chromatograms obtained at various temperatures after the reduction pulse are shown in Fig. 4. It is seen that all folding intermediates except for N and four des intermediates were reduced to R and/or 1S at all temperatures. By integrating peaks of the intermediates and comparing the peak areas before and after the reduction pulse, accurate populations of the des intermediates as well as N and 3S could be determined. It should be noted that the populations thus obtained did not change at all by increasing the time of the reduction pulse up to 8 min, indicating that N and the des intermediates were not reduced under the applied conditions. It is also notable that small peaks of des[26–84] and des[58–110] were clearly observed in the HPLC chromatogram at a reaction temperature of 25 °C after the reduction pulse. This indicates that these des intermediates have stable structures at 25 °C and pH 8.0 although their populations are very low. The presence of des[26–84] and des[58–110] during oxidative folding of RNase A under these conditions has not been proposed previously.

Fig. 5 shows the plots of the populations of 3S and four des intermediates determined by application of the reduction pulse at 5 °C and pH 8.0 as a function of the folding time (30 min–28 h). On the basis of the SS rearrangement schemes shown in Eqs. (1)–(4), we analyzed kinetics and thermodynamics of the reactions to obtain the first-order rate constants (k^{f}_{1-4} and k^{r}_{1-4}) and the equilibrium constants (K_{1-4}) at each temperature. The results are summarized in Table 1.

The values of K_{1-4} were determined by using populations of 3S, des[40–95], des[65–72], des[26–84], and des[58–110] after a long

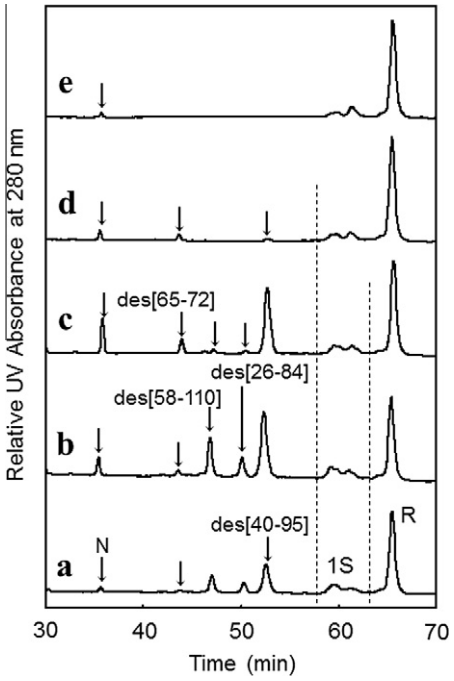

Fig. 4. HPLC chromatograms obtained by the reduction pulse experiments for RNase A using DTT^{red} as a reductant at pH 8.0. Folding conditions are the same as (a–e) of Fig. 2. The reduction pulse conditions: (a) 9 mM DTT^{red} for 4 min at 5 °C, (b) 8 mM DTT^{red} for 3 min at 15 °C, and (c–e) 7 mM DTT^{red} for 2 min at 25, 35, and 45 °C, respectively. See the text for details of the HPLC analysis conditions.

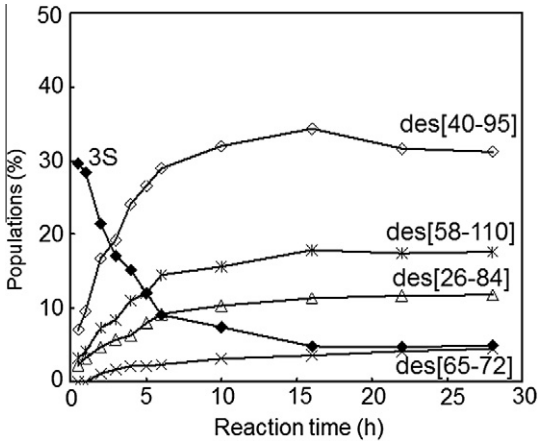

Fig. 5. Populations of the 3S and four des intermediates as a function of the reaction time. Reaction conditions were $[R]_0 = [DHS^{ox}]_0/3 = 14.0$ μM at 5 °C and pH 8.0.

period of the reaction time (16, 14, 10, and 8 h at 5, 15, 25, and 35 °C, respectively), where the pseudo-equilibriums attained. Free-energy differences of the des intermediates (ΔG) calculated by using the equilibrium constants and the temperature are also listed in Table 1. Des[40–95] is the most stable among the four des intermediates at 25 °C and the lower temperatures at pH 8.0. However, des[65–72] becomes more stable than des[40–95] at 35 °C.

On the other hand, the values of the first-order rate constants were determined as follows. First, the forward rate constants were estimated by using the relative population data obtained in the beginning of the incubation, where only forward reactions would take place because of low populations of the des intermediates. Second, given the equilibriums of Eqs. (1)–(4), the reverse rate constants were calculated by using the values of k^{f} and K. The kinetic data thus obtained revealed that the rates of formation (k^{f}_{1-4}) for the des intermediates from 3S increase in the order, des[65–72] < des[26–84] < des[58–110] < des[40–95], while the rates for the reverse reactions (k^{r}_{1-4}) fall in a narrow range of the magnitude at 5 and 15 °C. At 25 °C, the rate constants could be obtained accurately only for des[40–95] and des[65–72] because yields of the other des intermediates were quite low. At 35 °C, the rate constants could not be determined even for des[40–95] and des[65–72].

3.4. Formation of native structure

UV spectra of the solutions containing a mixture of R and three equivalents of DHS^{ox} were measured under the same reaction conditions to the oxidative folding experiments of RNase A in order to estimate ratios of the native structure regenerated during the incubation. From the magnitude of the absorbance change at 287 nm from that observed after 1 min of the incubation time, the native ratio could be estimated by using the $\Delta\varepsilon_{U \rightarrow N}$ value at 287 nm (1640 mol^{-1} cm^{-1}) determined by the SS-intact heat denaturation study at pH 8.0. The estimation relies on the observations that only a marginal amount of the native state (N) and des intermediates was accumulated within 1 min of the reaction mixture (as mentioned earlier) and also that the UV spectrum of the mixture of 1S–4S intermediates at pH 8.0 is similar to the SS-intact denatured state (U) [42]. However, since the conformation of the des intermediates would be looser than N, the native ratio thus obtained could be slightly underestimated. Fig. 6 compares ratios of the native structure generated after 5 h at various temperatures. Regenerated native ratios, which were determined by UV spectral analysis at 287 nm, and total populations of N and the des intermediates,

Table 1
Kinetic and thermodynamic parameters for the equilibriums between 3S and four des intermediates of RNase A at pH 8.0.

SS rearrangement	Temperature (°C)	k ($\times 10^3$ min^{-1})[f,a]	k^r ($\times 10^3$ min^{-1})[b]	$[des]_\infty$ (%)[c]	K[d]	ΔG (kcal/mol)[e]
3S ⇌ des[40–95]	5	4.8 ± 0.4	0.7 ± 0.1	32.4 ± 1.9	6.8 ± 0.5	−1.1 ± 0.1
	15	5.0 ± 0.3	0.7 ± 0.2	39.9 ± 1.1	7.0 ± 1.6	−1.1 ± 0.1
	25	9.1 ± 3.5	6.3 ± 0.7	29.4 ± 1.9	1.4±0.2	−0.2 ± 0.1
	35	ND[f]	ND	1.4 ± 0.4	0.03 ± 0.01	2.1 ± 0.3
3S ⇌ des[65–72]	5	0.6 ± 0.1	0.7 ± 0.1	4.1 ± 0.5	0.9 ± 0.1	0.1 ± 0.1
	15	1.0 ± 0.1	1.4 ± 0.4	4.2 ± 0.4	0.7 ± 02	0.2 ± 0.2
	25	1.3 ± 0.1	3.3 ± 0.5	8.3 ± 0.8	0.4 ± 0.1	0.5 ± 0.2
	35	ND	ND	2.7 ± 0.2	0.06 ± 0.01	1.7 ± 0.1
3S ⇌ des[26–84]	5	1.0 ± 0.4	0.4 ± 0.1	11.6 ± 0.2	2.4 ± 0.1	−0.5 ± 0.1
	15	1.3 ± 0.2	1.0 ± 0.2	7.5 ± 0.2	1.3 ± 0.3	−0.2 ± 0.1
	25	ND	ND	1.2 ± 0.4	0.06 ± 0.02	1.7 ± 0.2
	35	ND	ND	ND	ND	ND
3S ⇌ des[58–110]	5	2.2 ± 0.5	0.6 ± 0.1	17.7 ± 0.2	3.7 ± 0.1	−0.7 ± 0.1
	15	3.2 ± 0.2	1.8 ± 0.5	11.9 ± 1.7	2.1 ± 0.7	−0.4 ± 0.2
	25	ND	ND	1.1 ± 0.1	0.05 ± 0.01	1.8 ± 0.1
	35	ND	ND	ND	ND	ND

[a] Rate constants for formation of the des intermediates from the 3S intermediate ensemble.
[b] Rate constants for rearrangement from the des intermediates to the 3S intermediate ensemble.
[c] Relative populations of the des intermediates in the 3S species after a long period of the reaction time.
[d] Equilibrium constants for the equilibriums between the 3S intermediate ensemble and the des intermediates. The values were calculated by using $[des]_\infty$ and $[3S]_\infty$ ($[3S]_\infty$ = 4.8 ± 0.1% at 5 °C, 5.7 ± 1.1% at 15 °C, 20.5 ± 1.0% at 25 °C, and 42.7 ± 1.9% at 35 °C).
[e] Free energy differences of the des intermediates with respect to the 3S intermediate ensemble.
[f] Not determined.

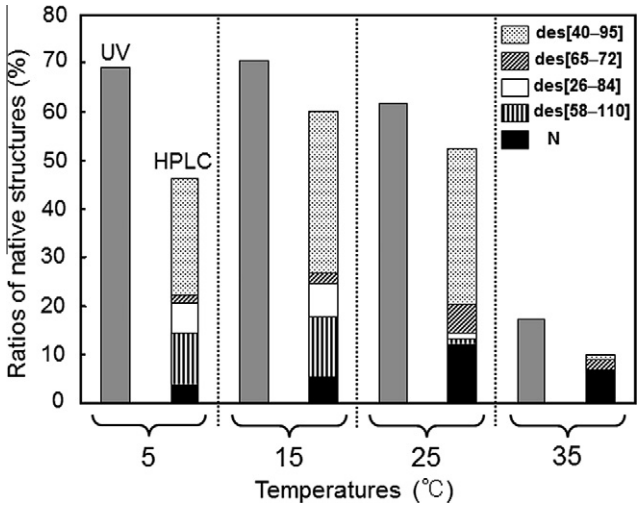

Fig. 6. Comparison of the ratios of native structure of RNase A estimated by UV measurement at 287 nm and those of the native state (N) and des intermediates at pH 8.0. Reaction conditions: $[R]_0 = [DHS^{ox}]_0/3$ = 25.1 μM at 5 °C, $[R]_0 = [DHS^{ox}]_0/3$ = 20.7 μM at 15 °C, $[R]_0 = [DHS^{ox}]_0/3$ = 24.7 μM at 25 °C, and $[R]_0 = [DHS^{ox}]_0/3$ = 23.7 μM at 35 °C. The reaction time was 300 min.

which were determined by reduction pulse experiments, well agree to each other, but the native ratios determined by UV are always larger. The difference is even enhanced at low temperatures.

3.5. Oxidation pulse

After incubation of the reaction mixture of R and three equivalents of DHS^{ox} at pH 8.0 and 15 °C for 300 min, one equivalent of DHS^{ox} was added to the reaction solution. The obtained HPLC chromatogram is shown in Fig. 7. Since DHS^{ox} is a strong oxidant, the oxidation pulse should convert R, 1S, 2S, and 3S without rigid structure to 4S. According to the pathways shown in Fig. 1, des[65–72] and des[40–95] would also be oxidized to N, while des[26–84] and des[58–110] would not be oxidized. Indeed, after the oxidation pulse, populations of N and 4S largely increased, and none of R, 1S, 2S, 3S, and des[65–72] was observed in the chromatogram although a small amount of des[40–95] remained. The increased ratio for N agreed well with the disappeared ratios for des[65–72] and des[40–95]. In the meantime, populations of des[26–84] and des[58–110] did not change by the oxidation pulse. The results clearly demonstrated that des[26–84] and des[58–110] are dead-end intermediates at 15 °C on the folding pathways of RNase A. This feature was explained previously by the residual cysteinyl SH groups of des[26–84] and des[58–110] being buried in the native-like folded structures [21].

3.6. Folding from isolated des intermediates to N

In addition to oxidation pulse experiments, four des intermediates were isolated in a form with the two SH groups unblocked, and their folding behaviors in a folding buffer solution were investigated at pH 8.0 and 5 °C in order to elucidate folding pathways from each des intermediate to N unambiguously. The sample solution obtained from the reduction pulse experiment was acidified at pH 2, and the acid-quenched des intermediates were separated and purified by reverse-phase HPLC (see supporting information). Each des intermediate was then dissolved in 1 mM HCl under an air atmosphere, and the folding reaction was initiated by increasing the pH to 8 to encourage SS formation by air oxidation and SS reshuffling. The sample solution was incubated at 5 °C for 300 min. The folding intermediates generated were monitored by HPLC with AEMTS quenching. Fig. 8 shows HPLC chromatograms obtained by folding of des[58–110], which is a dead-end intermediate at the temperature on the oxidative folding pathways of RNase A. The sample for the reaction time of 0 min was prepared by quenching the isolated des intermediate by AEMTS in 200 mM acetate buffer at pH 4.0. It is seen that ca. 40% of des[58–110] was converted to unfolded 3S species in 5 min and des[40–95] and des[65–72] were subsequently generated accompanying formation of N. Since des[58–110] cannot be directly oxidized to N according to the oxidation pulse experiment (Fig. 7), it is clear that des[40–95] and des[65–72], which were formed from des[58–110] via 3S, were subsequently transformed to N by air oxidation. Similar results were obtained in the folding of isolated des[26–84] (see supporting information). In contrast, in the folding of des[40–95]

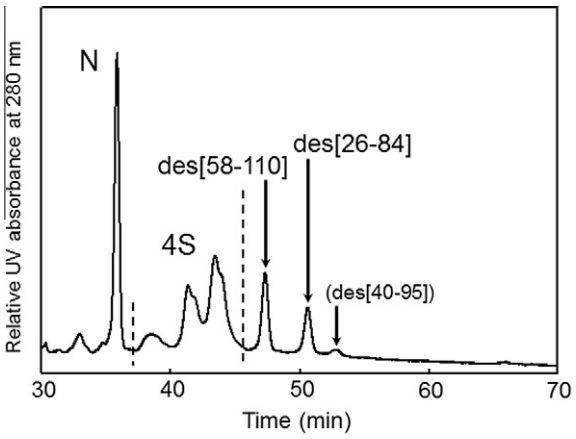

Fig. 7. An HPLC chromatogram obtained by the oxidation pulse experiment of RNase A at 15 °C and pH 8.0. Reaction conditions: $[R]_0 = [DHS^{ox}]_0/3 = 20.7$ μM. Oxidation pulse conditions: After 300 min of the refolding reaction, the sample solution was treated with one equivalent of DHS^{ox} at 15 °C for 3 min. See the text for details of the HPLC analysis conditions.

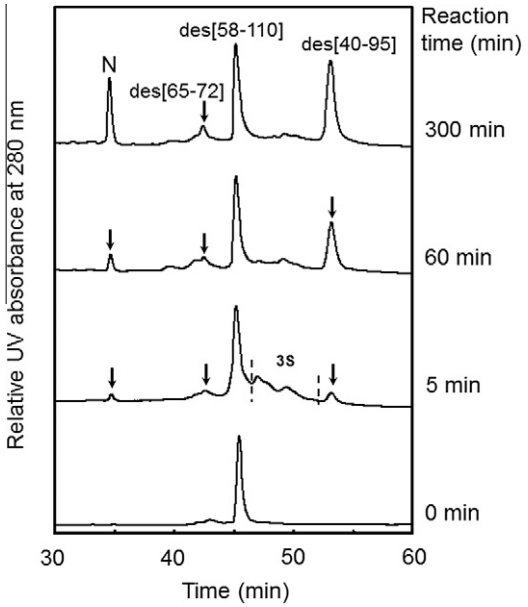

Fig. 8. HPLC chromatograms obtained by folding of isolated des[58–110] under an aerobic condition at pH 8.0 and 5 °C. The initial concentration of des[58–110] was approx. 20 μM.

and des[65–72], generation of des[26–84] and des[58–110] were not observed, and N was formed directly by air oxidation during the incubation.

4. Discussion

4.1. DHS^{ox} as a useful oxidative folding reagent

Oxidative folding pathways of RNase A were previously elucidated as shown in Fig. 1 [19–21], in which four des intermediates with native-like fold are located as key intermediates. These des intermediates could be observed only by carrying out well-designed experiments. For example, des[40–95] and des[65–72] were characterized by initiation of the refolding reaction by reacting R with a large excess amount of an oxidant, such as DTT^{ox}, followed by the incubation for a controlled period of time, removal of the redox species (i.e., DTT^{ox} and DTT^{red}), and then incubation of the obtained mixture of folding intermediates again in an appropriate buffer solution [19]. Des[26–84] and des[58–110] were characterized by application of a reduction pulse of DTT^{red} to the folding mixture of R and DTT^{ox} obtained at 15 °C after enough progression of the oxidative folding reaction [20].

On the other hand, we observed in this study the four des intermediates very easily just by mixing R with an appropriate amount of DHS^{ox} as shown in Fig. 2. This was possible because DHS^{ox} is a strong and selective oxidant for SS formation, hence the oxidant is not left in the folding mixture after 1 min even at 5 °C. Meanwhile, the observation that the des intermediates were detected apparently only when three equivalents of DHS^{ox} were employed clearly indicated that the des intermediates are dominantly generated from the 3S intermediate ensemble via SS rearrangement. The result from the oxidation pulse experiment (Fig. 7) further demonstrated that among the four des intermediates des[40–95] and des[65–72] can be oxidized to N at 15 °C. Thus, the oxidative folding pathways of RNase A were fully reproduced in a simple manner by using DHS^{ox}. It was previously shown that DHS^{ox} is useful as a strong and quantitative SS formation reagent for reduced proteins at a wide pH range (at least 3–10) [41,42]. The present study further reveals that DHS^{ox} works as a rapid and quantitative oxidant at pH 8.0 in a wide range of temperature at least from 5 to 45 °C.

In the oxidative folding protocol applied here, the reduced protein (R) was just mixed with an appropriate amount of DHS^{ox} at a controlled pH and temperature. This simple method allowed us not only to assign the exact folding pathways but also to obtain precise thermodynamic and kinetic parameters as to the key folding intermediates as given in Table 1. Detailed thermodynamic and kinetic features of the des intermediates as well as the whole folding pathways toward the native state (N) are discussed below.

4.2. Thermodynamics of the des intermediates

Equilibriums (Eqs. (1)–(4)) were established between 3S and the four des intermediates after long-time incubation of the reaction mixture of R and DHS^{ox} (Fig. 5). The reversible changes in the populations observed in the temperature-jump experiment (Fig. 3) unequivocally confirmed the presence of the equilibriums. Therefore, the relative populations of the des intermediates obtained after long-time incubation should reflect their thermodynamic stabilities. It should be noted, however, that the equilibriums are not real ones because des[40–95] and des[65–72] are slowly oxidized to N, even in the absence of DHS^{ox}, via intermolecular SH–SS exchange reactions [54].

At 5 and 15 °C, the equilibrium constants (K) showed that des[40–95] is most stable and the thermodynamic stability decreases in order of des[40–95], des[58–110], des[26–84], and des[65–72]. The free-energy differences between the most stable des[40–95] and the least stable des[65–72] at 5 and 15 °C were 1.2 and 1.3 kcal/mol, respectively (Table 1). Such quantitative thermodynamic data for all the des intermediates were first determined in this study.

At higher temperatures, however, the stability order changed significantly: des[65–72] becomes more stable than des[58–110] and des[26–84] at 25 °C, and it becomes most stable at 35 °C. According to the reduction pulse experiments (Fig. 4), des[58–110] and des[26–84] were observed at the temperature up to 25 °C, while des[40–95] and des[65–72] could be observed till 35 °C. These observations strongly suggest that denaturation temperatures (T_m) of des[40–95] and des[65–72] are higher than those of des[58–110] and des[26–84]. Indeed, it was previously reported that 3SS mutants of RNase A lacking one native SS linkage, i.e., [C40A, C95A], [C65A, C72A], [C26A, C84A], and [C58A, C110A], denature at 34, 39, 27, and 24 °C, respectively [27–29], which is

consistent with the fact that the populations of des[40–95], des[65–72], des[26–84], and des[58–110] significantly decrease at 25–35, 35–45, 15–25, and 15–25 °C, respectively. Thus, a loss of relative populations for the four des intermediates by raising a temperature is reflected by the denaturation temperatures.

Although des[65–72] would have the highest T_m value, its stability at low temperatures (5 and 15 °C) was the lowest among the four des intermediates. Similarly, des[58–110] is more stable than des[26–84] below 15 °C but the T_m of des[58–110] would be lower than that of des[26–84] according to the denaturation study of the 3SS mutants [27]. Thus, it appeared that there is no direct correlation between relative thermodynamic stabilities of the des intermediates and the T_m values. This feature would indicate that each native SS linkage of RNase A plays different roles in the thermodynamic and kinetic properties. C65–C72 should have the largest effect on thermodynamic stability of the native structure, whereas C26–C84 and C58–C110, which are buried inside of the folded native structure, would be more important than the other SS linkages for the kinetic stability.

4.3. Kinetics of the des intermediates

The rate constants for the conversion from the 3S intermediate ensemble to des[40–95] and des[65–72] at 25 °C and pH 8.0 were previously estimated by Scheraga and coworkers as 0.014 and 0.0021 min^{-1}, respectively, based on the oxidative folding study of RNase A by using DTT^{ox} as an oxidant [55]. The corresponding values obtained in this study are 0.0091 and 0.0013 min^{-1}, respectively (Table 1). Although the values are a little small compared with previous ones, the both values would be roughly consistent with each other by considering large experimental errors. On the other hand, for the reverse reactions from des[40–95] and des[65–72] to 3S, the rate constants previously determined were 0.0064 and 0.0003 min^{-1}, respectively, based on the reductive unfolding study of RNase A by using an excess amount of DTT^{red} [56], while the corresponding values obtained in this study were 0.0063 and 0.0033 min^{-1}. The values for the conversion of des[40–95] are in good agreement with each other. However, those for the conversion of des[65–72] are in significant difference. The discrepancy is likely due to difference in the experimental conditions: previous rate constants were determined for the irreversible reactions from the des intermediates to specific 3S intermediates (i.e., 3S′, direct precursors of the des intermediates), not for the reversible reactions between 3S and the des intermediates as performed in this study.

Based on the forward rate constants obtained for Eqs. (1)–(4) (k^f_{1-4}), time constants (τ) of the reactions were calculated to be τ = 110 min for des[40–95] and 770 min for des[65–72] at 25 °C, while τ = 200 min for des[40–95], 1000 min for des[65–72], 770 min for des[26–84], and 310 min for des[58–110] at 15 °C. Thus, it turned out that native structure formation in the oxidative folding of RNase A progresses in a long time-scale (100–1000 min) at around room temperatures. On the other hand, conformational folding of SS-intact RNase A rapidly proceeds for the unfolded species of U_{vf+f} (19%), U_m (9%), U^{II}_s (58%), and U^{I}_s (13%) in time-scales of 28 ms, 1.6, 23, and 120 s, respectively, under favorable folding conditions at 0.58 M GdnHCl, pH 5.0, and 15 °C [57]. The folding processes, which are controlled by X-Pro peptidyl cis–trans isomerization, are very rapid compared to the conformational folding processes observed in the oxidative folding. This may suggest that the native structure formation accompanied by SS rearrangement was not associated with X-Pro isomerization but with other structuring processes. However, it would not be necessarily correct because the rate constants (k^f_{1-4}) obtained in this study are based on the reaction from the entire 3S intermediate ensemble to the des intermediates. In precise treatment, 3S should contain various SS species.

Since we observed only four des intermediates as structured 3S species in the reduction pulse experiment, it would be obvious that formation of the three native SS linkages precedes folding to the native structure as shown in Eq. (5),

$$\underbrace{\ldots \rightleftharpoons 3S'' \rightleftharpoons 3S' \rightleftharpoons \mathrm{desU}}_{3S} \overset{k^{f\prime}}{\rightleftharpoons} \mathrm{des\ N} \tag{5}$$

where desU and desN are the des intermediates with unfolded and folded conformation, respectively. Thus, in the oxidative folding of RNase A the conformational folding process would take place at least after formation of the three native SS linkages, being consistent with the previous model suggested by Scheraga and coworkers [45,47,58]. Based on the reaction scheme of Eq. (5), the step from desU to desN should correspond to a conformational folding process to the native structure, and the formation rate of desN from 3S intermediate ensemble must become very slow due to a low population of desU.

To assess the chemical events involved in the rate-determining process of the desN formation (Eq. (5)), we subsequently calculated activation energies for the conversion from 3S to des[40–95] and des[65–72] by Arrhenius plots using the forward rate constants (k^f) at three different temperatures (5, 15, and 25 °C). The obtained values were 5 ± 4 and 6 ± 2 kcal/mol for 3S → des[40–95] and 3S → des[65–72], respectively. For des[26–84] and des[58–110], the accurate activation energies could not be determined due to a lack of the k^f values at 25 °C. However, the roughly estimated values by using the data at 5 and 15 °C were 4 and 6 kcal/mol, respectively, which are similar to those obtained for des[40–95] and des[65–72]. Interestingly, these values are also similar to the activation energies reported for refolding of SS-intact RNase A at 0.58 M GdnHCl, pH 5.0, and 15 °C (8 ± 4 and 4 ± 2 kcal/mol for the unfolded species of U_{vf+f} and U^{II}_s, respectively) [57]. The agreement strongly suggested that the events involved in the rate-determining process of the 3S → desN in the SS-coupled RNase A folding are the X-Pro isomerization processes similarly to those involved in the SS-intact folding. Thus, it is most likely that the bottleneck of the formation of desN (Eq. (5)) is the conformational folding step from desU to desN coupled with X-Pro isomerization, not the SS reshuffling among 3S species. Indeed, it was previously reported that the time-scale for folding of unfolded des[40–95] is significantly longer than that for the SS reshuffling to 3S at pH 8.0 and 25 °C [47].

As X-Pro cis–trans isomerization processes would be involved in the $k^{f\prime}$ process of Eq. (5), populations of desU in the 3S species (% desU) were subsequently estimated by using the following equation:

$$v = k^f[3S] = k^{f\prime}[\mathrm{desU}] \tag{6}$$

where v is the reaction rate for formation of the des intermediates. Assuming that the $k^{f\prime}$ values under the conditions of the present study (i.e., at 0 M GdnHCl, pH 8.0, and 15 °C) are similar to the folding rate constants for SS-intact RNase A determined at 0.58 M GdnHCl, pH 5.0, and 15 °C [57], we estimated that the % desU values should be very small (<1%, <0.2%, <0.3%, and <0.7% for des[40–95], des[65–72], des[26–84], and des[58–110], respectively).

4.4. Regeneration pathways toward the native state (N)

The oxidative folding pathways of RNase A consist of three phases (Fig. 1), which can be clearly separated by employing DHS^{ox} [40]. A whole spectrum of a time course for oxidative folding of RNase A when three equivalents of DHS^{ox} were applied as an oxidant at 25 °C and pH 8.0 is shown in Fig. 9, where the data obtained from three different experiments were combined to connect the time course. The short-term data were obtained by the method

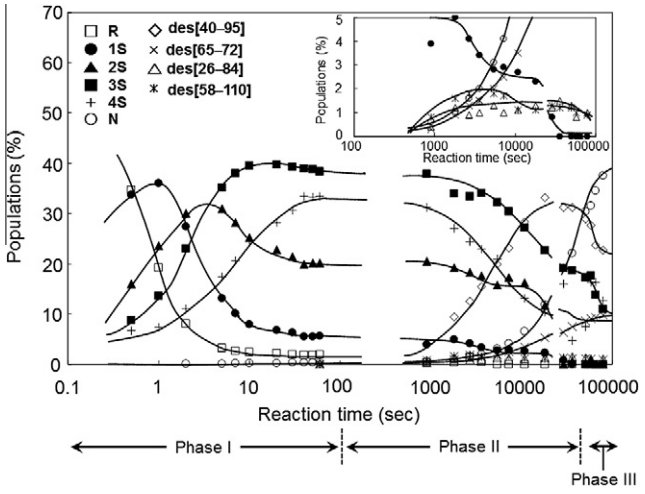

Fig. 9. A whole time course for oxidative folding of RNase A by using DHS^{ox} as an oxidant at pH 8.0 and 25 °C. Reaction conditions: $[R]_0 = [DHS^{ox}]_0/3 = 48.0$ μM for phase I, $[R]_0 = [DHS^{ox}]_0/3 = 26.4$ μM for phase II, $[R]_0 = [DHS^{ox}]_0/3 = 17.0$ μM for phase III. The relative populations of 1S, N, and des intermediates are expanded in an inset.

using a quench-flow instrument as described before [40]. This kind of clear separation of the folding phases is only possible by using a strong oxidant, such as DHS^{ox}. Each separated phase would be important in building up the native structures to reach the final destination.

Phase I is a SS formation (oxidation) process to lose the chain entropy. This phase makes the conformational space to search for N significantly limited. The produced 1S–4S intermediates as well as R do not have stable folded structure, although accumulation of some weak native interactions and hydrophobic clustering was evidenced previously for 1S–4S intermediates of RNase A [42]. When DHS^{ox} is applied as an oxidant, the reaction completes in a short time range (~1 min). If there is no rigid folded structure, the reaction would become a stochastic reaction, meaning that the reaction rates are simply proportional to the number of SH groups present along a polypeptide chain [40,42,43].

Phase II is a conformational folding process via SS rearrangement to gain the native folded structures. This process should proceed via desU species, which would fold to the native structure through X-Pro cis–trans isomerization. Fig. 6 shows that the total amount of N and the des intermediates generated in phase II is not enough to explain the UV absorbance change at 287 nm, suggesting generation of some intermediates having weakly folded structures other than the four des intermediates. One of the candidates for such intermediates would be the 2S intermediate with C58–C110 and C26–C84 SS bonds [59], which would populate more at low temperatures. Nevertheless, those intermediates are difficult to be observed due probably to the low populations as well as the facile reduction to R under the reduction pulse conditions. The SS rearrangement proceeds in a time-scale of 1 min–1 d at pH 8.0.

Phase III is a final oxidation step to generate N. According to the result from an oxidation pulse experiment (Fig. 7), it is obvious that N dominantly formed through des[40–95] and des[65–72]. As seen in Figs. 2 and 4, N was slowly generated during incubation of the folding mixture at pH 8.0 via intermolecular SH–SS exchange reactions [54]. The population of N after 5 h increased with raising the temperature and became maximum at 25 °C. The change synchronizes with the relative populations of des[40–95] and des[65–72], confirming that these des intermediates are productive intermediates on the oxidative folding pathways of RNase A. The time-scale of this final phase is very long (>1 d) in the absence of an excess amount of an oxidant.

Moreover, by using DHS^{ox} we have succeeded in direct observation of the transformation processes from each isolated des intermediate to N in the present study. In the conventional oxidative folding method using DTT^{ox} as an oxidant, des[26–84] and des[58–110] could not be isolated due to the low populations in the folding buffer solution. This is because fast oxidation of des[40–95] and des[65–72] to N by excess DTT^{ox} present in the solution shifts the equilibriums between the four des intermediates (Eqs. (1)–(4)) toward des[40–95] and des[65–72]. On the other hand, when DHS^{ox} was used as a redox reagent, the oxidant did not remain during slow SS rearrangement processes (i.e., phase II). Under low temperature conditions (5–15 °C), therefore, all four des intermediates achieved the equilibriums depending on their thermodynamic stability. As a result, each des intermediate was obtained at a relatively high population. In the folding of isolated des[40–95] and des[65–72], they were preferentially oxidized to N rather than converted to 3S under an aerobic condition at pH 8.0 and 5 °C. This suggested that des[40–95] and des[65–72] have robust folded structures against the SS reshuffling process leading to 3S intermediates. In contrast, in the folding of isolated des[26–84] and des[58–110] they were gradually converted to des[40–95] and des[65–72] through 3S. Thus, it was evidenced that the two dead-end intermediates have more flexible structures to unfold to 3S than the other des intermediates. The results are consistent with the consequence that the two SS linkages of Cys26–Cys84 and Cys58–Cys110, which are buried in the native structure, would play a role in the kinetic stability.

Meanwhile, N was still generated in a small amount at 45 °C even though the des intermediates were not observed at the temperature (Fig. 4e). Under such high temperature conditions, folded des species (desN) are no longer stable, and fast equilibriums should be established between desU and 3S. Therefore, generation of N would be accomplished by prompt acquirement of the native conformation after oxidation of desU via intermolecular SH–SS exchange reactions or probably air oxidation. Such pathways to N via unstructured intermediates are similar to the main folding pathways observed for hirudin mutant HV-1 [60] and 3SS mutants of RNase A lacking C40–C95 or C65–C72 SS bridges [22,23].

5. Conclusions

By application of DHS^{ox} as an oxidative folding reagent, all four possible des intermediates (des[40–95], des[65–72], des[26–84], and des[58–110]) of RNase A could be clearly and easily characterized. This was possible due to the fact that the oxidant (i.e., DHS^{ox}) is not left in the folding mixture after 1 min even at 5 °C because SS formation is completed rapidly and quantitatively by using DHS^{ox}. The folding protocol applied here was much easier to identify the oxidative folding pathways than previous methods using sulfur oxidants, such as DTT^{ox} and GSSG. This simple method allowed us not only to assign the major folding pathways exactly but also to obtain quantitative thermodynamic and kinetic parameters as to the key folding intermediates.

After quantitative SS formation in a short time-scale (<1 min) by addition of three equivalents of DHS^{ox}, the four des intermediates were slowly generated by SS rearrangement from the 3S intermediate ensemble. The amounts of these des intermediates generated after a long reaction time at low temperatures depended on the thermodynamic stabilities. Although des[65–72] was thermodynamically least stable at 5–15 °C, the T_m was highest among the four des intermediates. This indicated that there is no direct correlation between thermodynamic stability and T_m for the four des intermediates, suggesting that each native SS linkage of RNase A

plays different roles in the thermodynamic and kinetic properties: C65–C72 should have the largest effect on thermodynamic stability of the native structure, whereas C26–C84 and C58–C110 would be more important than the other SS linkages for the kinetic stability. Moreover, kinetic analysis for the four des intermediates was carried out. The k^f and E_a parameters obtained for the reactions of 3S → des suggested that the reaction proceeds through desU species, which would gain the native structure via X-Pro isomerization. Thus, SS-intact conformational folding processes of RNase A may be applied to the second phase (phase II) of the SS-coupled conformational folding. Furthermore, by taking advantage of DHS^{ox} all four des intermediates on the oxidative folding pathways could be populated and isolated by acid quenching. Oxidative folding of each des intermediate clearly confirmed the pathways to N. Des[26–84] and des[58–110] cannot be directly oxidized to N but can be preferentially converted to 3S by SS reshuffling, whereas des[40–95] and des[65–72] can be dominantly oxidized to N.

By employing DHS^{ox}, three phases of the oxidative folding of RNase A (Fig. 1) could be clearly separated with respect to a time course (Fig. 9). This facile strategy using DHS^{ox} would be an efficient approach toward elucidation of oxidative folding mechanisms of various SS-containing proteins. Such studies are being conducted in our laboratory to obtain common features of oxidative protein folding pathways.

Acknowledgment

This work was supported by the Ministry of Education, Culture, Sports, Science and Technology of Japan (Grant-in-Aid for Scientific Research (C): No. 23550198).

Appendix A. Supplementary data

Supplementary data associated with this article can be found, in the online version, at http://dx.doi.org/10.1016/j.fob.2012.04.001.

References

[1] Saven, J.G. (2001) Designing protein energy landscapes. Chem. Rev. 101, 3113–3130.
[2] Pepys, M.B. (2006) Amyloidosis. Annu. Rev. Med. 57, 223–241.
[3] Daggett, V. and Fersht, A.R. (2003) Is there a unifying mechanism for protein folding? Trends Biochem. Sci. 28, 18–25.
[4] Welker, E., Maki, K., Shastry, M.C.R., Juminaga, D., Bhat, R., Scheraga, H.A. and Roder, H. (2004) Ultrarapid mixing experiments shed new light on the characteristics of the initial conformational ensemble during the folding of ribonuclease A. Proc. Natl. Acad. Sci. USA 101, 17681–17686.
[5] Chang, J.Y. (2009) Structural heterogeneity of 6 M GdmCl-denatured protein: implications for the mechanism of protein folding. Biochemistry 48, 9340–9346.
[6] Ewbank, J.J. and Creighton, T.E. (1991) The molten globule protein conformation probed by disulfide bonds. Nature 350, 518–520.
[7] Creighton, T.E. (1997) How important is the molten globule for correct protein folding? Trends Biochem. Sci. 22, 6–10.
[8] Chowdhury, F.A., Fairman, R., Bi, Y., Rigotti, D.J. and Raleigh, D.P. (2004) Protein dissection experiments reveal key differences in the equilibrium folding of α-lactalbumin and the calcium binding lysozymes. Biochemistry 43, 9961–9967.
[9] Creighton, T.E. and Goldenberg, D.P. (1984) Kinetic role of a meta-stable native-like two-disulfide species in the folding transition of bovine pancreatic trypsin inhibitor. J. Mol. Biol. 179, 497–526.
[10] Mücke, M. and Schmid, F.X. (1994) Folding mechanism of ribonuclease T1 in the absence of the disulfide bonds. Biochemistry 33, 14608–14619.
[11] van den Berg, B., Chung, E.W., Robinson, C.V. and Dobson, C.M. (1999) Characterization of the dominant oxidative folding intermediate of hen lysozyme. J. Mol. Biol. 290, 781–796.
[12] Arolas, J.L., Aviles, F.X., Chang, J.Y. and Ventura, S. (2006) Folding of small disulfide-rich proteins: clarifying the puzzle. Trends Biochem. Sci. 31, 292–301.
[13] Weissman, J.S. and Kim, P.S. (1991) Reexamination of the folding of BPTI: predominance of native intermediates. Science 253, 1386–1393.
[14] Anderson, W.L. and Wetlaufer, D.B. (1976) The folding pathway of reduced lysozyme. J. Biol. Chem. 251, 3147–3153.
[15] Ewbank, J.J. and Creighton, T.E. (1993) Structural characterization of the disulfide folding intermediates of bovine α-lactalbumin. Biochemistry 32, 3694–3707.
[16] Chatrenet, B. and Chang, J.Y. (1993) The disulfide folding pathway of hirudin elucidated by stop/go folding experiments. J. Biol. Chem. 268, 20988–20996.
[17] Rothwarf, D.M. and Scheraga, H.A. (1993) Regeneration of bovine pancreatic ribonuclease A. 1. Steady-state distribution. Biochemistry 32, 2671–2679.
[18] Raines, R.T. (1998) Ribonuclease A. Chem. Rev. 98, 1045–1065.
[19] Rothwarf, D.M., Li, Y.J. and Scheraga, H.A. (1998) Regeneration of bovine pancreatic ribonuclease A: identification of two nativelike three-disulfide intermediates involved in separate pathways. Biochemistry 37, 3760–3766.
[20] Welker, E., Narayan, M., Volles, M.J. and Scheraga, H.A. (1999) Two new structured intermediates in the oxidative folding of RNase A. FEBS Lett. 460, 477–479.
[21] Welker, E., Narayan, M., Wedemeyer, W.J. and Scheraga, H.A. (2001) Structural determinants of oxidative folding in proteins. Proc. Natl. Acad. Sci. USA 98, 2312–2316.
[22] Xu, X. and Scheraga, H.A. (1998) Kinetic folding pathway of a three-disulfide mutant of bovine pancreatic ribonuclease A missing the [40–95] disulfide bond. Biochemistry 37, 7561–7571.
[23] Iwaoka, M., Juminaga, D. and Scheraga, H.A. (1998) Regeneration of three-disulfide mutants of bovine pancreatic ribonuclease A missing the 65–72 disulfide bond: characterization of a minor folding pathway of ribonuclease A and kinetic roles of Cys65 and Cys72. Biochemistry 37, 4490–4501.
[24] Wu, J., Yang, Y. and Watson, J.T. (1998) Trapping of intermediates during the refolding of recombinant human epidermal growth factor (hEGF) by cyanylation, and subsequent structural elucidation by mass spectrometry. Protein Sci. 7, 1017–1028.
[25] Narayan, M., Welker, E. and Scheraga, H.A. (2003) Native conformational tendencies in unfolded polypeptides: development of a novel method to assess native conformational tendencies in the reduced forms of multiple disulfide-bonded proteins. J. Am. Chem. Soc. 125, 2036–2037.
[26] Iwaoka, M., Wedemeyer, W.J. and Scheraga, H.A. (1999) Conformational unfolding studies of three-disulfide mutants of bovine pancreatic ribonuclease A and the coupling of proline isomerization to disulfide redox reactions. Biochemistry 38, 2805–2815.
[27] Klink, T.A., Woycechowsky, K.J., Taylor, K.M. and Raines, R.T. (2000) Contribution of disulfide bonds to the conformational stability and catalytic activity of ribonuclease A. Eur. J. Biochem. 267, 566–572.
[28] Shimotakahara, S., Ríos, C.B., Laity, J.H., Zimmerman, D.E., Scheraga, H.A. and Montelione, G.T. (1997) NMR structural analysis of an analog of an intermediate formed in the rate-determining step of one pathway in the oxidative folding of bovine pancreatic ribonuclease A: automated analysis of ^{1}H, ^{13}C, and ^{15}N resonance assignments for wild-type and [C65S, C72S] mutant forms. Biochemistry 36, 6915–6929.
[29] Laity, J.H., Lester, C.C., Shimotakahara, S., Zimmerman, D.E., Montelione, G.T. and Scheraga, H.A. (1997) Structural characterization of an analog of the major rate-determining disulfide folding intermediate of bovine pancreatic ribonuclease A. Biochemistry 36, 12683–12699.
[30] Annis, I., Chen, L. and Barany, G. (1998) Novel solid-phase reagents for facile formation of intramolecular disulfide bridges in peptides under mild conditions. J. Am. Chem. Soc. 120, 7226–7238.
[31] Gough, J.D., Williams Jr, R.H., Donofrio, A.E. and Lees, W.J. (2002) Folding disulfide-containing proteins faster with an aromatic thiol. J. Am. Chem. Soc. 124, 3885–3892.
[32] Gough, J.D., Gargano, J.M., Donofrio, A.E. and Lees, W.J. (2003) Aromatic thiol pK_a effects on the folding rate of a disulfide containing protein. Biochemistry 42, 11787–11797.
[33] Shi, T. and Rabenstein, D.L. (2002) Discovery of a highly selective and efficient reagent for formation of intramolecular disulfide bonds in peptides. J. Am. Chem. Soc. 122, 7226–7238.
[34] Narayan, M., Welker, E., Wanjalla, C., Xu, G. and Scheraga, H.A. (2003) Shifting the competition between the intramolecular reshuffling reaction and the direct oxidation reaction during the oxidative folding of kinetically trapped disulfide-insecure intermediates. Biochemistry 42, 10783–10789.
[35] Beld, J., Woycechowsky, K.J. and Hilvert, D. (2007) Selenoglutathione: efficient oxidative protein folding by a diselenide. Biochemistry 46, 5382–5390.
[36] Beld, J., Woycechowsky, K.J. and Hilvert, D. (2010) Diselenides as universal oxidative folding catalysts of diverse proteins. J. Biotechnol. 150, 481–489.
[37] Lyles, M.M. and Gilbert, H.F. (1991) Catalysis of the oxidative folding of ribonuclease A by protein disulfide isomerase: dependence of the rate on the composition of the redox buffer. Biochemistry 30, 613–619.
[38] Lyles, M.M. and Gilbert, H.F. (1991) Catalysis of the oxidative folding of ribonuclease A by protein disulfide isomerase: pre-steady-state kinetics and the utilization of the oxidizing equivalents of the isomerase. Biochemistry 30, 619–625.
[39] Cabrele, C., Fiori, S., Pegoraro, S. and Moroder, L. (2002) Redox-active cyclic bis(cysteinyl)peptides as catalysts for in vitro oxidative protein folding. Chem. Biol. 9, 731–740.
[40] Iwaoka, M., Kumakura, F., Yoneda, M., Nakahara, T., Henmi, K., Aonuma, H., Nakatani, H. and Tomoda, S. (2008) Direct observation of conformational folding coupled with disulphide rearrangement by using a water-soluble selenoxide reagent – a case of oxidative regeneration of ribonuclease A under weakly basic conditions. J. Biochem. 144, 121–130.

[41] Iwaoka, M. and Tomoda, S. (2000) *trans*-3,4-Dihydroxy-1-selenolane oxide: a new reagent for rapid and quantitative formation of disulfide bonds in polypeptides. Chem. Lett. 1400–1401.
[42] Arai, K., Kumakura, F. and Iwaoka, M. (2010) Characterization of kinetic and thermodynamic phases in the prefolding process of bovine pancreatic ribonuclease A coupled with fast SS formation and SS reshuffling. Biochemistry 49, 10535–10542.
[43] Arai, K., Dedachi, K. and Iwaoka, M. (2011) Rapid and quantitative disulfide bond formation for a polypeptide chain using a cyclic selenoxide reagent in an aqueous medium. Chem. Eur. J. 17, 481–485.
[44] Talluri, S., Rothwarf, D.M. and Scheraga, H.A. (1994) Structural characterization of a three-disulfide intermediate of ribonuclease a involved in both the folding and unfolding pathways. Biochemistry 33, 10437–10449.
[45] Cao, A., Welker, E. and Scheraga, H.A. (2001) Effect of mutation of proline 93 on redox unfolding/folding of bovine pancreatic ribonuclease A. Biochemistry 40, 8536–8541.
[46] Welker, E., Wedemeyer, W.J., Narayan, M. and Scheraga, H.A. (2001) Coupling of conformational folding and disulfide-bond reactions in oxidative folding of proteins. Biochemistry 40, 9059–9064.
[47] Saito, K., Welker, E. and Scheraga, H.A. (2001) Folding of a disulfide-bonded protein species with free thiol(s): competition between conformational folding and disulfide reshuffling in an intermediate of bovine pancreatic ribonuclease A. Biochemistry 40, 15002–15008.
[48] Boudko, S.P. and Engel, J. (2004) Structure formation in the C terminus of Type III collagen guides disulfide cross-linking. J. Mol. Biol. 335, 1289–1297.
[49] Lu, D. and Liu, Z. (2008) Dynamic redox environment-intensified disulfide bond shuffling for protein refolding in vitro: molecular simulation and experimental validation. J. Phys. Chem. B 112, 15127–15133.
[50] Iwaoka, M., Takahashi, T. and Tomoda, S. (2001) Syntheses and structural characterization of water-soluble selenium reagents for the redox control of protein disulfide bonds. Heteroatom Chem. 12, 293–299.
[51] Bruice, T.W. and Kenyon, G.L. (1982) Novel alkyl alkanethiolsulfonate sulfhydryl reagents. Modification of derivatives of L-cysteine. J. Protein Chem. 1, 47–58.
[52] Welker, E., Hathaway, L. and Scheraga, H.A. (2004) A new method for rapid characterization of the folding pathways of multidisulfide-containing proteins. J. Am. Chem. Soc. 126, 3720–3721.
[53] Xu, X., Rothwarf, D.M. and Scheraga, H.A. (1996) Nonrandom distribution of the one-disulfide intermediates in the regeneration of ribonuclease A. Biochemistry 35, 6406–6417.
[54] Song, M.C. and Scheraga, H.A. (2000) Formation of native structure by intermolecular thiol-disulfide exchange reactions without oxidant in the folding of bovine pancreatic ribonuclease A. FEBS Lett. 471, 177–181.
[55] Rothwarf, D.M., Li, Y.J. and Scheraga, H.A. (1998) Regeneration of bovine pancreatic ribonuclease A: detailed kinetic analysis of two independent folding pathways. Biochemistry 37, 3767–3776.
[56] Li, Y.J., Rothwarf, D.M. and Scheraga, H.A. (1995) Mechanism of reductive protein unfolding. Nat. Struct. Mol. Biol. 2, 489–494.
[57] Houry, W.A. and Scheraga, H.A. (1996) Nature of the unfolded state of ribonuclease A: effect of cis-trans X-Pro peptide bond isomerization. Biochemistry 35, 11719–11733.
[58] Narayan, M., Welker, E., Wedemeyer, W.J. and Scheraga, H.A. (2000) Oxidative folding of proteins. Acc. Chem. Res. 33, 805–812.
[59] Lester, C.C., Xu, X., Laity, J.H., Shimotakahara, S. and Scheraga, H.A. (1997) Regeneration studies of an analog of ribonuclease A missing disulfide bonds 65–72 and 40–95. Biochemistry 36, 13068–13076.
[60] Thannhauser, T.W., Rothwarf, D.M. and Scheraga, H.A. (1997) Kinetic studies of the regeneration of recombinant hirudin variant 1 with oxidized and reduced dithiothreitol. Biochemistry 36, 2154–2165.